

Heat Capacities and Low Temperature Thermal Transitions of 1-Hexyl and 1-Octyl-3-methylimidazolium bis(trifluoromethylsulfonyl)amide

Thomas J. Hughes,* Tauqir Syed, Brendan F. Graham, Kenneth N. Marsh, and Eric F. May

Centre for Energy, School of Mechanical and Chemical Engineering, University of Western Australia, Crawley WA, 6009 Australia

S Supporting Information

ABSTRACT: Several previous measurements of the isobaric heat capacity of the ionic liquid 1-hexyl-3-methylimidazolium bis(trifluoromethylsulfonyl)amide ([Hmim][Tf₂N]) differ relative to the IUPAC recommended value by $\pm 8\%$. Specifically, the results obtained by differential scanning calorimetry (DSC) showed relative difference from each other and from values determined by adiabatic calorimetry by up to 12% and by 6% on average. The aim of this work was to explore the reason for these discrepancies in DSC measurements. Accordingly, measurements of the isobaric heat capacity and low temperature thermal transitions of [Hmim][Tf₂N] and 1-octyl-3-methylimidazolium bis(trifluoromethylsulfonyl)amide ([Omim][Tf₂N]) made by DSC are reported here. The isobaric heat capacities for both ionic liquids were measured on samples of (5 to 9) g over the temperature ranges (303 to 373) K for [Hmim][Tf₂N] and (288 to 373) K for [Omim][Tf₂N] using steps of 10 K and a scan rate of 0.025 K·min⁻¹. These heat capacity measurements were consistent, within their estimated relative uncertainty of 3%, with the values measured by adiabatic calorimetry and with the DSC measurements made at scan rates of less than 1 K·min⁻¹ on samples of 5 g or greater. In addition, several thermal transitions were observed for these ionic liquids at temperatures down to 140 K. For [Hmim][Tf₂N] a melting temperature of (272 \pm 1) K and an enthalpy of fusion of (62 \pm 2) J·g⁻¹ were measured, which are consistent within the combined uncertainties with those of Shimizu et al. (*J. Phys. Chem. B* **2006**, *110*, 13970–13975). After tempering the [Omim][Tf₂N] sample, a melting temperature of (250 \pm 1) K and an enthalpy of fusion of (58 \pm 2) J·g⁻¹ was obtained, which differ by 1.6 K and 3.7% respectively from values reported by Paulechka et al. (*J. Chem. Thermodyn.* **2007**, *39*, 866–877).

INTRODUCTION

Ionic liquids are commonly defined as organic salts that have melting temperatures of less than 373 K. They have a range of properties that may make them useful replacements for volatile organic solvents such as their extremely low vapor pressure, nonflammability, and in many cases low toxicity.¹ Reviews by Zhao,¹ Plechkova and Seddon,² and Werner et al.³ describe the present industrial processes which use ionic liquids and discuss many other possible industrial applications of ionic liquids. To evaluate their use in such processes the thermophysical properties of ionic liquids need to be well understood. In 2002 IUPAC launched project 2002-005-1-100 entitled *Thermodynamics of ionic liquids, ionic liquid mixtures, and the development of standardized systems*. An objective of the IUPAC project was to make reference quality measurements of important thermophysical properties of the selected ionic liquid to establish recommended reference values of these properties. The reference ionic liquid selected was 1-hexyl-3-methylimidazolium bis(trifluoromethylsulfonyl)amide ([Hmim][Tf₂N]) and a “IUPAC” sample of this liquid was prepared and distributed to all researchers participating in the project.⁴

Heat capacity is a particularly important property for process design, and Paulechka⁵ has recently published a critical review of ionic liquid heat capacities. For [Hmim][Tf₂N] three sets of heat capacity measurements were collected as part of the initial IUPAC study.⁴ Heat capacities of the IUPAC sample of liquid [Hmim][Tf₂N] were measured using adiabatic calorimetry by Shimizu et al.⁶ and Blokhin et al.⁷ and using differential scanning calorimetry (DSC) by Archer.⁸ In addition, all three groups

measured the heat capacity of crystalline [Hmim][Tf₂N] phases and its enthalpy of fusion. The IUPAC recommended values for the heat capacities and enthalpy of fusion were published by Chirico et al.⁹ In addition to the IUPAC commissioned measurements, Crosthwaite et al.,¹⁰ Diedrichs and Gmehling,¹¹ and Ge et al.¹² published measurements of the heat capacity of [Hmim][Tf₂N] made using DSC. A summary of the literature data and the measurement details is given in Table 1. Chirico et al. noted that there were “surprisingly large” deviations between the IUPAC recommended values and other measurements using DSC. The relative difference from the IUPAC recommended heat capacity of the DSC measurements of Crosthwaite et al., Diedrichs and Gmehling, Archer, and Ge et al. were -7% , (2 to 5)%, (0.5 to 6)%, and (3 to 6.5)%, respectively.¹³ A possible contributing factor to these large deviations was the method of measurement including factors such as the scan rate and sample size. For each measurement set, Table 1 lists the sample mass, scan rate, DSC method, as well as the DSC instrument used for the measurements. As a result of these large differences in the DSC results, one of us (K.N.M.) acting as the IUPAC project chair requested two additional sets of DSC measurements to try and resolve the discrepancies. Recently, one set of those additional measurements, corresponding to the temperature range (323 to 573) K, was reported by Bochmann and Hefter.¹⁴ The purpose of this paper is to report the results of the second set of DSC measurements made over the lower temperature range (300 to 373) K.

Received: November 11, 2010

Accepted: January 20, 2011

Published: February 24, 2011

Table 1. Scan Rates, Sample Mass, Calorimeter Manufacturer, Method, and Estimated Relative Standard Uncertainty for Literature Heat Capacity Measurements by DSC of Liquid [Hmim][Tf₂N] and [Omim][Tf₂N]

author	β^a	m_{sample}	T range	manufacturer	DSC method	u_r^f
	K min ⁻¹	mg	K			
Archer ^{8,b}	5	2 to 15	196 to 370	TA Instruments DSC-2920	continuous scan	6 %
Bochmann and Hefter ¹⁴	0.25	^c	325 to 564	Setaram C80	5 K steps	
Bochmann and Hefter ¹⁴	1	^c	325 to 564	Setaram C80	20 K steps	0.7 %
Bochmann and Hefter ¹⁴	0.5	^c	325 to 564	Setaram C80	10 K steps	
Crosthwaite et al. ^{10,b}	10	20 to 50 ^d	298, 323	Mettler-Toledo DSC822	continuous scan	11 %
Diedrichs and Gmehling (1) ^{11,b}	0.15	5000 to 8000	318 to 418	Setaram BT 2.15	continuous scan	5 %
Diedrichs and Gmehling (2) ^{11,b}	20	5 to 10	320 to 425	TA Instruments DSC Q100	continuous scan	5 %
Diedrichs and Gmehling (3) ^{11,b}	2 ^e	5 to 10	323 to 423	TA Instruments DSC Q100	modulated DSC ^e	5 %
Ge et al. ¹²	20	5 to 10	293 to 358	TA Instruments DSC Q100	continuous scan	12 %

^a β represents the scan rate. ^bWork includes measurements of [Hmim][Tf₂N] only. ^cVolumetric heat capacities were measured with a calorimetry cell volume of ≈ 15 mL. ^dFrom Fredlake et al.²² ^e2 K·min⁻¹, temperature amplitude of ± 0.531 K, 100 s modulation period. ^fRelative standard uncertainty estimates from Paulechka.⁵

Table 2. Mass Fraction of Water, w , in Ionic Liquids Measured by Coulometric Karl Fischer Titration prior and after Calorimetry

	run 1 prior 10 ⁶ w	run 2 prior 10 ⁶ w	run 1 after 10 ⁶ w	run 2 after 10 ⁶ w
[Hmim][Tf ₂ N]	13	4	not measured	103
[Omim][Tf ₂ N]	7	4	not measured	4

In addition, measurements of the heat capacity and enthalpy of fusion of 1-octyl-3-methylimidazolium bis(trifluoromethylsulfonyl)amide [Omim][Tf₂N] are reported here, again over a complementary temperature range to that of Bochmann and Hefter.¹³ Prior to these two new studies, the discrepancies in the reported heat capacity measurements of [Omim][Tf₂N] were more problematic than for [Hmim][Tf₂N] because all three existing data sets were inconsistent. The heat capacities measured using DSC by Crosthwaite et al.⁹ were 5 % lower relative to those reported by Paulechka et al.¹⁷ using adiabatic calorimetry. Subsequent DSC measurements reported in 2008 by Ge et al.¹¹ were on average a further 8 % larger relative to the values of Paulechka et al.¹⁷ A summary of the available literature heat capacity data for [Omim][Tf₂N] is also given in Table 1.

EXPERIMENTAL SECTION

Apparatus. Heat capacities and enthalpies of thermal transitions were measured using a differential Setaram BT 2.15 Tian-Calvet heat flow calorimeter.^{15,16} This calorimeter utilizes liquid nitrogen for cooling and can operate between (77 and 473) K. The power detection threshold of the calorimeter was between (2 and 20) μ W depending on the sample and scanning rate. The sensitivity of the calorimeter's heat flux sensor varies between (18 and 34) μ V·mW⁻¹ depending on the temperature. The heat flux sensor was calibrated using electrically heated Joule cells provided by Setaram.

Materials. Samples of [Hmim][Tf₂N] and [Omim][Tf₂N] were prepared at the University of Canterbury New Zealand and transported under a nitrogen atmosphere to the University of Western Australia. Prior to the measurements, about 50 cm³ of ionic liquid was added to a custom drying and storage flask with a magnetic mixing bar. The liquid was stirred with the magnetic mixer and heated in an oven to 343 K while a vacuum of (10 to 30) Pa was applied.

After about 48 h the vacuum pump was switched off and the flask was flushed with dry nitrogen. Samples were then taken via the flask's septum for Karl Fischer titration (Metrohm 831 Coulometer). Two samples of both [Hmim][Tf₂N] and [Omim][Tf₂N] were used in the calorimetric measurements. The mass fractions of water in these samples, measured before and after the measurements, are listed in Table 2.

Heat Capacity Measurements. In early experiments samples of ionic liquid were taken by syringe out of the storage flask and injected in to a dry N₂ flushed standard 8 mL stainless steel calorimeter cell. Dry N₂ was flowed into the top of the cell for about a minute before the cell's lid was closed, compressing an O-ring seal. In later experiments the transfer technique was further refined to minimize exposure to moisture in the air. A 10 mL syringe flushed with dry nitrogen was used to remove samples of the dried ionic liquid from the flask. The syringe was then placed inside a glovebag with a dry N₂ atmosphere. The sample cell was similarly flushed and placed inside the glovebag. Finally with both the syringe and the cell inside the glovebag, the sample was injected into the cell, which was then sealed. In all of the experiments, the calorimeter's reference cell was filled with dry nitrogen.

Heat capacity measurements were made using the step technique described by the manufacturer and by Bochmann and Hefter.¹⁴ Samples were equilibrated for 5.5 h initially and also following each 10 K temperature step, during which the rate of heating was 0.025 K·min⁻¹. The mass of each sample is listed in Table 3. Heat capacities of the ionic liquids were calculated from

$$c_p = \frac{\int \Phi_s dt - \int \Phi_b dt}{m\Delta T_{\text{step}}} \quad (1)$$

where $\int \Phi_s dt$ is the integrated heat flow difference between the cell with sample and the reference cell containing dry N₂ over the

Table 3. Masses of Ionic Liquids Used in Experiments^a

	run 1	run 2	low temperature transitions
	<i>m</i> /g	<i>m</i> /g	<i>m</i> /g
[Hmim][Tf ₂ N]	9.404 ± 0.001	5.7238 ± 0.0001	11.7613 ± 0.0002
[Omim][Tf ₂ N]	5.454 ± 0.001	5.5846 ± 0.0001	5.5846 ± 0.0001

^a Masses listed are the true masses. The density used to calculate the true mass for [Hmim][Tf₂N] was from taken from the equation provided in the review of Chirico et al.,⁹ and for [Omim][Tf₂N] was taken from Tokuda et al.²³ The size of the buoyancy correction was approximately 0.072 % and 0.076 % for [Hmim][Tf₂N] and [Omim][Tf₂N], respectively.

Table 4. Enthalpies of Fusion and Melting Temperatures of Water and Mercury

$\beta/\text{K}\cdot\text{min}^{-1}$	0.025	0.050	0.075	reference	this work	reference
	$\Delta_{\text{fus}}h/\text{kJ}\cdot\text{kg}^{-1}$	$\Delta_{\text{fus}}h/\text{kJ}\cdot\text{kg}^{-1}$	$\Delta_{\text{fus}}h/\text{kJ}\cdot\text{kg}^{-1}$	$\Delta_{\text{fus}}h/\text{kJ}\cdot\text{kg}^{-1}$	T_{fus}/K	T_{fus}/K
water	342.88	345.89	347.04	333.5 ± 0.2 ¹⁹	273.09	273.15
mercury	11.563	11.568	11.554	11.471 ± 0.005 ¹⁸	234.18	234.3210 ± 0.0005 ¹⁷

temperature step, $\int \Phi_b dt$ is the integrated heat flow difference for a scan where both the sample and reference cells were filled with dry N₂, *m* is the sample mass, and ΔT_{step} is the temperature step interval.

Low Temperature Transitions and Enthalpy of Fusion Measurements. The heat flow measurements made during the scans of the low temperature transitions are shown in Figures S1, S2, and S3 of the Supporting Information (SI). The [Hmim][Tf₂N] sample was first cooled to 148.15 K overnight. Its temperature was then rapidly increased to 223.15 K where it was held constant for several hours before the sample was heated at a rate of 0.025 K·min⁻¹ from (223.15 to 298.15) K (Figure S1). In another experiment, a sample of [Omim][Tf₂N] was cooled to 148.15 K and held at that temperature for 2 h. The sample was then heated at a rate of 0.08 K·min⁻¹ from (148.15 to 323.15) K (Figure S2). An exothermic event occurred just below the melting temperature and consequently the two enthalpy peaks overlapped. Subsequently, the same sample of [Omim][Tf₂N] was cooled to 223.15 K and held there for 4 h before being heated at 0.03 K·min⁻¹ to 238.15 K where the sample was tempered for about 12 h to ensure the glass phase transition was completed. The sample was then cooled to and maintained at 223.15 K for another 8 h before it was heated at a rate of 0.03 K·min⁻¹ from (223.15 to 278.15) K (Figure S2). This avoided the problem of overlapping peaks and allowed the enthalpy of fusion to be determined reliably. The buoyancy corrected true mass of both the [Hmim][Tf₂N] and [Omim][Tf₂N] samples are listed in Table 3. The enthalpy of fusion, $\Delta_{\text{fus}}h$, was calculated from

$$\Delta_{\text{fus}}h = \int \Phi_s dt / m \quad (2)$$

where $\int \Phi_s dt$ is the integrated heat flow difference between the cell with sample and the reference cell containing dry N₂ over the fusion peak and *m* is the mass of the sample.

Uncertainty Estimation. To test the calorimeter's performance and the sample thermometer's calibration, enthalpy of fusion measurements were conducted with deionized water and with mercury at scan rates, β , of (0.025, 0.050, and 0.075) K·min⁻¹. The temperature ranges of the scans were (253.15 to 288.15) K for water and (213.15 to 248.15) K for mercury. The onset temperature as a function of the scan rate is shown in

Figure S4a and S4b of the SI for water and mercury, respectively. The extrapolated onset temperature for a scan rate of zero was (273.10 ± 0.03) K and (234.18 ± 0.02) K for water and mercury, respectively, compared to the ice point of 273.15 K for water and recommended melting temperature of 234.3210 K for mercury.¹⁷ All onset temperatures measured in this work for the ionic liquid samples were corrected for scan-rate dependence by (3.4 β) K, where the multiplier is the average of the slopes shown in Figure S4 for water and mercury. The enthalpies of fusion measured for water and mercury are given in Table 4 and were 3.7 % and 0.8 % higher relative to their respective reference values.^{18,19} The water was not degassed and this could have affected the $\Delta_{\text{fus}}H$ determination.

The van't Hoff equation²⁰

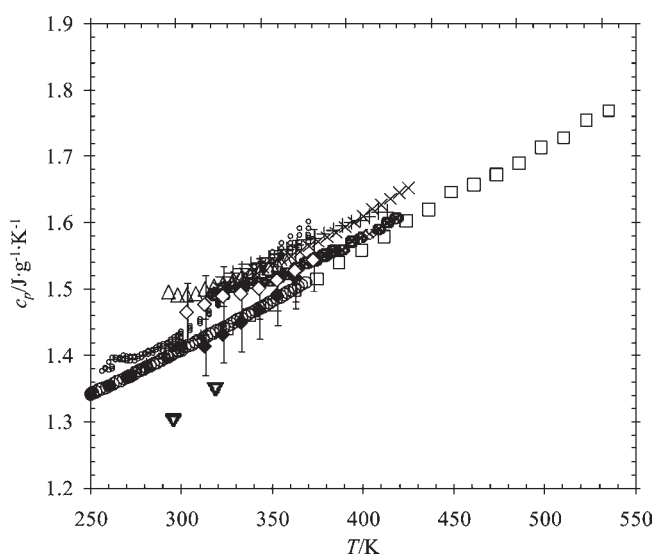
$$T = T_0 - x(RT_0^2/\Delta_{\text{fus}}H_m)1/f \quad (3)$$

provides a method for calculating the freezing point depression. Here T_0 is the melting temperature of the pure substance, *x* is the mole fraction of impurity in the liquid solution, $\Delta_{\text{fus}}H_m$ is the molar enthalpy of fusion, and *f* is the fraction of the solid melted. Assuming that the liquid phase is an ideal solution and that the impurities do not form a solid solution, it is possible to estimate the level of impurities in the sample from a DSC enthalpy fusion peak using eq 1.²⁰ The purities of the [Hmim][Tf₂N] and [Omim][Tf₂N] samples were estimated from the enthalpy of fusion scans, where the fraction melted as a function of temperature was calculated from the cumulative area fraction of the enthalpy of fusion peak by the calorimeter's Calisto software (see Laye²⁰). The leading slope of a mercury enthalpy of fusion peak (73 mW·K⁻¹) at the same scan rate as the ionic liquid fusion scans was used to correct for the effects of thermal lag. Fitting the van't Hoff equation from (5 and 25) % of the fusion peak area gave mole fraction purities of 0.9985 and 0.9902 for the [Hmim][Tf₂N] and [Omim][Tf₂N] samples, respectively.

From the enthalpy of fusion and purity analyses, we estimate that the relative combined uncertainty, $u_{c,r}$, at a 95 % confidence limit in the enthalpies of fusion to be about ± 3 % and the standard uncertainty in the temperature to be ± 0.25 K. We estimate that the relative standard uncertainty in the heat capacity measured by the step method is also likely to be about ± 3 %.

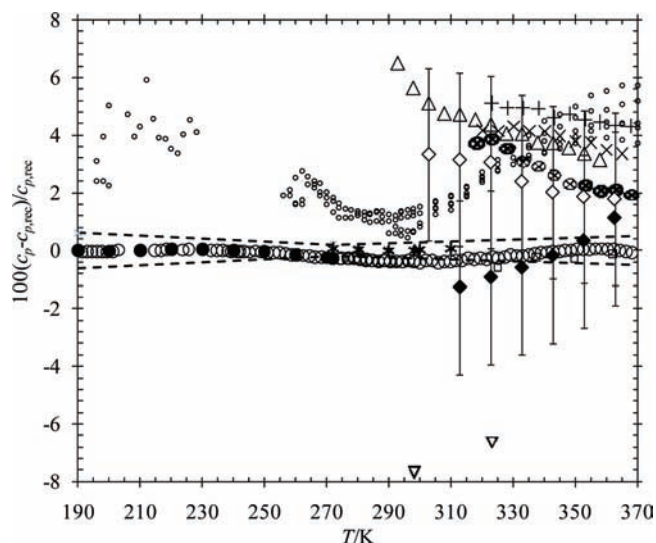
Table 5. Experimental Isobaric Heat Capacities of [Hmim][Tf₂N], $u(T) = 0.25$ K, $u_r(c_p) = 3$ %

run 1		run 2	
T	c_p	T	c_p
K	J·g ⁻¹ ·K ⁻¹	K	J·g ⁻¹ ·K ⁻¹
312.83	1.413	302.86	1.465
322.81	1.431	312.83	1.476
332.78	1.449	322.79	1.489
342.76	1.468	332.76	1.492
352.72	1.489	342.73	1.500
362.68	1.517	352.70	1.512
372.64	1.543	362.67	1.527
		372.64	1.543

**Figure 1.** Isobaric heat capacity of [Hmim][Tf₂N] as a function of temperature, \blacklozenge , this work – run 1; \lozenge , this work – run 2; ∇ , Crosthwaite et al.;^{10*}, Shimizu et al.;⁶ circle with \times , Diedrichs and Gmehling (1);¹¹ \times , Diedrichs and Gmehling (2);¹¹ $+$, Diedrichs and Gmehling (3);¹¹ \circ , Archer;⁸ \bullet , Blokhin et al. (1);⁷ \circ , Blokhin et al. (2);⁷ Δ , Ge et al.;¹² \square , Bochmann and Hefter.¹⁴

RESULTS AND DISCUSSION

Heat Capacities. The measured heat capacities of [Hmim][Tf₂N] are listed in Table 5 and are compared to literature values in Figure 1. Figure 2 shows a deviation plot of the heat capacities from the IUPAC recommended values. These recommended values by Chirico et al.⁹ are in the form of a weighted least-squares polynomial fit to the adiabatic calorimetry data of Shimizu et al.⁶ and Blokhin et al.⁷ as well as the DSC data of Archer⁸ between (190 to 370) K. Our heat capacities are within 3 % (estimated standard relative uncertainty $u_r = 3$ %) of the recommended values for all but three of the measurements. We note that the data set of Diedrich and Gmehling (3)¹¹ was measured with a Setaram BT 2.1S, the same as used in this study, and that their data closely matches our data. Diedrich and Gmehling measured the heat capacity over the whole temperature range by a continuous scans method, in which three sets of scans were

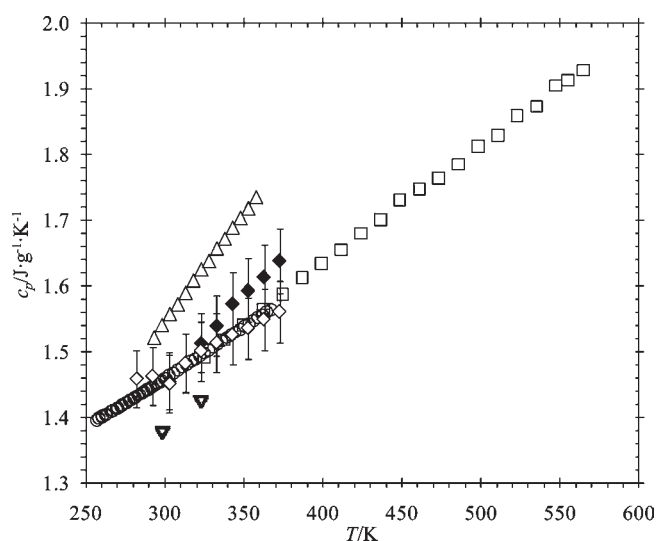
**Figure 2.** Deviation plot for [Hmim][Tf₂N] isobaric heat capacity from the IUPAC recommended values (Chirico et al.⁹), \blacklozenge , this work – run 1; \lozenge , this work – run 2; ∇ , Crosthwaite et al.;^{10*}, Shimizu et al.;⁶ circle with \times , Diedrichs and Gmehling (1);¹¹ \times , Diedrichs and Gmehling (2);¹¹ $+$, Diedrichs and Gmehling (3);¹¹ \circ , Archer;⁸ \bullet , Blokhin et al. (1);⁷ \circ , Blokhin et al. (2);⁷ Δ , Ge et al.;¹² \square , Bochmann and Hefter.¹⁴ The combined expanded uncertainty in the IUPAC recommended values is represented by the dashed lines.

performed against the reference cell, one with the ionic liquid, one with N₂, and one with α -Al₂O₃ as the calibration substance. Bochmann and Hefter¹⁴ measured the volumetric heat capacities at 10 MPa using three sets of step scans with a Setaram C80 heat flow Tian-Calvet calorimeter. Dry N₂ was used in the reference cell and water was used as a calibration substance in the sample cell. The cell and connecting tube was completely filled with the sample and at 1 cm above the cell the tubing was heated to 1 K above the cell temperature to limit heat transfer up the tube. Steps of 5 and 20 K were used at two different scan rates. We note that Bochmann and Hefter's heat capacity data closely matches the adiabatic data and appears to have a similar slope with temperature. Diedrich and Gmehling's, Bochmann and Hefter's, and our data were all collected with relatively large sample masses of more than 5 g and with slow scan rates of less than 1 K·min⁻¹. Other DSC data sets, namely Crosthwaite et al.,¹⁰ Diedrichs and Gmehling data sets (2) and (3), Archer,⁸ and Ge et al.¹² were measured with small sample sizes of less than 50 mg and scan rates between (2 and 20) K·min⁻¹. Archer's data generally agree well with the values obtained using adiabatic calorimetry but at both the lower and higher temperature extremes of the scan, the relative difference increases to almost 6%. In general the DSC data with smaller samples and faster scan rates are higher by up to 8%, from the adiabatic measurements and those measured with a DSC with a large sample and slow scan rate. (The DSC data of Crosthwaite et al.¹⁰ are an exception being 7% lower than the adiabatic values.)

The heat capacities of [Omim][Tf₂N] measured in this work are listed in Table 6 and are compared to literature values in Figure 3. Figure 4 shows a deviation plot of the heat capacities from recommended values given in a recent critical review by Paulechka.⁵ Paulechka fitted literature data which he had assigned a relative standard uncertainty of less than 2.5 % (refer to Table 1) to a polynomial by weighted least-squares between (188 and 370) K. As for the [Hmim][Tf₂N] measurements our heat

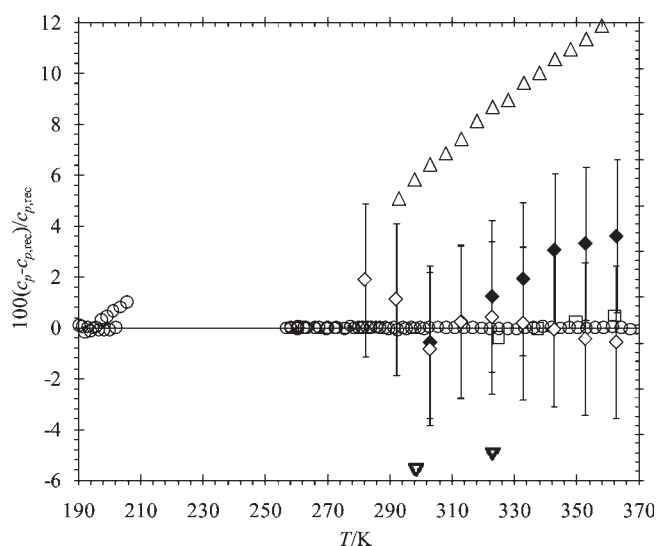
Table 6. Experimental Isobaric Heat Capacities of [Omim][Tf₂N], $u(T) = 0.25$ K, $u_r(c_p) = 3$ %

run 1		run 2	
T	c_p	T	c_p
K	J·g ⁻¹ ·K ⁻¹	K	J·g ⁻¹ ·K ⁻¹
302.88	1.455	281.99	1.458
312.86	1.483	291.95	1.462
322.84	1.513	302.86	1.451
332.81	1.540	312.83	1.482
342.78	1.573	322.79	1.501
352.74	1.593	332.76	1.513
362.71	1.614	342.72	1.525
372.66	1.639	352.68	1.535
		362.65	1.549
		372.62	1.560

**Figure 3.** Isobaric heat capacity of [Omim][Tf₂N] as a function of temperature, \blacklozenge , this work – run 1; \diamond , this work – run 2; ∇ , Crosthwaite et al.;¹⁰ \circ , Paulechka et al.;²¹ \triangle , Ge et al.;¹² \square , Bochmann and Hefter.¹⁴

capacities are consistent with the recommended values within our estimated experimental uncertainty. Bochmann and Hefter's¹⁴ DSC measurements of [Omim][Tf₂N] are also consistent with the adiabatic calorimetry measurements within the combined uncertainty. Again, DSC measurements with large sample mass and slow scan rates contrast with DSC results obtained with small samples and faster scan rates.

We conclude from both sets of measurements that sample masses greater than 5 g and slower scan rates, less than 2 K·min⁻¹ give more reliable heat capacities by DSC for ionic liquids. In particular the DSC technique used by Bochmann and Hefter gives heat capacity data that closely match the adiabatic values and have smaller scatter than other DSC measurements. Paulechka⁵ independently estimated the relative standard uncertainty of Bochmann and Hefter's heat capacity measurements to be 0.7%. The high quality of those DSC data is probably due to the use of a calibrant and the volumetric measurement technique where the volume or mass of the material is not required as it is

**Figure 4.** Deviation plot for [Omim][Tf₂N] isobaric heat capacity from the Paulechka's⁵ recommended values, \blacklozenge , this work; \diamond , repeat this work; ∇ , Crosthwaite et al.;¹⁰ \circ , Paulechka et al.;²¹ \triangle , Ge et al.;¹² \square , Bochmann and Hefter.¹⁴

accounted for by the calibration method. Furthermore, the step method is preferable to the continuous scan method commonly used in DSC measurements as it eliminates the problem of sample-furnace temperature lag which is particularly problematic with larger sample masses. It is also noted that in Bochmann and Hefter's technique the calorimetric cells were not removed between measurements, minimizing any effects of changes in cell orientation or surface contact with the calorimeter's furnace.

Low Temperature Thermal Transitions and Enthalpies of Fusion. Table 7 contains a summary of the enthalpy of fusion and melting temperatures measured in this work and reported by other workers for [Hmim][Tf₂N] and [Omim][Tf₂N]. The low temperature scan for [Hmim][Tf₂N] is shown in Figure S1. An event, possibly related to the completion of crystallization or a transition from a metastable to stable crystal structure, occurred at an onset temperature of 241.53 K. The ionic liquid melted at an onset temperature of 271.45 K with an enthalpy of fusion of 61.90 J·g⁻¹. The thermogram is similar to that given by Archer.⁸ Our enthalpy of fusion is about 2% relative lower than Shimizu et al.'s value (the IUPAC project recommended value), which is within the combined uncertainties, and our melting temperature is 0.32 K higher.

The low temperature scans for [Omim][Tf₂N] are presented in Figures S2 and S3. In Figure S2 a glass transition was observed at $T \approx 185$ K. Another transition, possibly an exothermic devitrification, occurred at an onset temperature of 230.11 K. In this scan, however the exothermic peak overlapped the enthalpy of fusion peak which is estimated to have an onset temperature of 250 K. For this reason a repeat scan was made after tempering as described in the Experimental Section. Figure S3 shows that for this scan the exothermic event was completely eliminated by tempering, allowing the enthalpy of fusion to be determined as 57.66 J·g⁻¹ with an onset temperature of 249.81 K. Our enthalpy of fusion is 3.7% lower relative to the value reported by Paulechka et al.²¹ for crystal structure III and our melting temperature is about 1.5 K lower. Both differences are greater than the combined uncertainties but Paulechka et al.²¹ notes that several crystal phases exist close to this temperature.

Table 7. Melting Temperatures and Enthalpies of Fusion of [Hmim][Tf₂N] and [Omim][Tf₂N] Crystal III

	T_{fus}	$\Delta_{\text{fus}}h$	method	
	K	kJ·kg ⁻¹		
[Hmim][Tf ₂ N]	271.45 ± 0.25	61.90 ± 1.86	DSC	this work
	271.13 ^a	63.34 ^a	AC	Shimizu et al. ⁶
	272.03 ± 0.01	62.78 ± 0.17	AC	Blokhin et al. ⁷ – crystal α
	272.03 ± 0.01	62.95 ± 0.08	AC	Blokhin et al. ⁷ – crystal β
	272.03 ± 0.01	63.20 ± 0.11	AC	Blokhin et al. ⁷ – crystal γ
	272.11 ± 0.29	62.20 ± 0.49	DSC	Archer ⁸
[Omim][Tf ₂ N]	249.81 ± 0.25	57.66 ± 1.73	DSC	this work
	251.42 ± 0.02	59.90 ± 0.27	AC	Paulechka et al. ²¹ – crystal III

^a Uncertainty not estimated by authors.

Paulechka et al.²¹ studied these different solid phases of [Omim][Tf₂N] with adiabatic calorimetry using different tempering techniques. They noted that crystal structure III is metastable compared to crystal structures I and II, which melt at (263.96 and 255.9) K, respectively.²¹

■ ASSOCIATED CONTENT

S Supporting Information. Thermograms of the low temperature transitions as well as plots of the onset temperature of the enthalpy of fusion for mercury and water as a function of scan rate. This material is available free of charge via the Internet at <http://pubs.acs.org>.

■ AUTHOR INFORMATION

Corresponding Author

*E-mail: thomas.hughes@uwa.edu.au.

■ ACKNOWLEDGMENT

We thank André Pinkert and John Boxall for preparing the ionic liquids used in this work.

■ REFERENCES

- Zhao, H. Innovative Applications of Ionic Liquids as “Green” Engineering Liquids. *Chem. Eng. Commun.* **2006**, *193*, 1660–1677.
- Plechko, N. V.; Seddon, K. R. Applications of Ionic Liquids in the Chemical Industry. *Chem. Soc. Rev.* **2008**, *37*, 123–150.
- Werner, S.; Marco, H.; Wasserscheid, P. Ionic Liquids in Chemical Engineering. *Annu. Rev. Chem. Biomol. Eng.* **2010**, *1*, 203–230.
- Project: Thermodynamics of Ionic Liquids, Ionic Liquid Mixtures, and the Development of Standardized Systems. <http://www.iupac.org/web/ins/2002-005-1-100>; accessed 31-Oct-10.
- Paulechka, Y. U. Heat Capacity of Room-Temperature Ionic Liquids: A Critical Review. *J. Phys. Chem. Ref. Data* **2010**, *39*, 033108/1–033108/23.
- Shimizu, Y.; Ohte, Y.; Yamamura, Y.; Saito, K.; Atake, T. Low-Temperature Heat Capacity of Room-Temperature Ionic Liquid, 1-Hexyl-3-methylimidazolium Bis(trifluoromethylsulfonyl)imide. *J. Phys. Chem. B* **2006**, *110*, 13970–13975.
- Blokhin, A. V.; Paulechka, Y. U.; Kobo, G. J. Thermodynamic Properties of [C₆mim][NTf₂] in the Condensed State. *J. Chem. Eng. Data* **2006**, *51*, 1377–1388.
- Archer, D. G. *Thermodynamic Properties of 1-hexyl-3-methylimidazolium bis(trifluoromethylsulfonyl)imide*; Internal Report-6645; National Institute of Standards and Technology: Gaithersburg, MD, 2006.

- Chirico, R. D.; Diky, V.; Magee, J. W.; Frenkel, M.; Marsh, K. N.; Rossi, M. J.; McQuillan, A. J.; Lynden-Bell, R. M.; Brett, C. M. A.; Dymond, J. H.; Goldbeter, A.; Hou, J. G.; Marquardt, R.; Sykes, B. D.; Yamanouchi, K. Thermodynamic and Thermophysical Properties of the Reference Ionic Liquid: 1-Hexyl-3-Methylimidazolium Bis[(trifluoromethyl)sulfonyl]amide (Including Mixtures). Part 2. Critical Evaluation and Recommended Property Values. *Pure Appl. Chem.* **2009**, *81*, 791–828.

- Crosthwaite, J. M.; Muldoon, M. J.; Dixon, J. K.; Anderson, J. L.; Brennecke, J. F. Phase Transition and Decomposition Temperatures, Heat Capacities and Viscosities of Pyridinium Ionic Liquids. *J. Chem. Thermodyn.* **2005**, *37*, 559–568.

- Diedrichs, A.; Gmehling, J. Measurement of Heat Capacities of Ionic Liquids by Differential Scanning Calorimetry. *Fluid Phase Equilib.* **2006**, *244*, 68–77.

- Ge, R.; Hardacre, C.; Jacquemin, J.; Nancarrow, P.; Rooney, D. W. Heat Capacities of Ionic Liquids as a Function of Temperature at 0.1 MPa. Measurement and Prediction. *J. Chem. Eng. Data* **2008**, *53*, 2148–2153.

- Marsh, K. N.; Brennecke, J. F.; Chirico, R. D.; Frenkel, M.; Heintz, A.; Magee, J. W.; Peters, C. J.; Rebelo, L. P. N.; Seddon, K. R.; Rossi, M. J.; McQuillan, A. J.; Lynden-Bell, R. M.; Brett, C. M. A.; Dymond, J. H.; Goldbeter, A.; Hou, J. G.; Marquardt, R.; Sykes, B. D.; Yamanouchi, K. Thermodynamic and Thermophysical Properties of the Reference Ionic Liquid: 1-Hexyl-3-Methylimidazolium Bis[(trifluoromethyl)sulfonyl]amide (Including Mixtures). Part 1. Experimental Methods and Results. *Pure Appl. Chem.* **2009**, *81*, 781–790.

- Bochmann, S.; Hefter, G. Isobaric Heat Capacities of the Ionic Liquids [C_nmim][Tf₂N] (n = 6, 8) from (323 to 573) K at 10 MPa. *J. Chem. Eng. Data* **2010**, *55*, 1808–1813.

- Low Temperature Calorimeter (from –196°C to 200°C), Setaram, Thermal Analysis and Calorimetry. <http://www.setaram.com/BT-2.15.htm>; accessed 11-Nov-10.

- Schaarschmidt, B. Setaram Calorimeters. In *Handbook of Thermal Analysis and Calorimetry Vol. 1: Principles and Practice*; Brown, M. E., Ed.; Elsevier: Burlington, MA, 1998; pp 618–634.

- Nicholas, J. V.; White, D. R. Temperature. In *IUPAC Experimental Thermodynamics Vol. VI: Measurement of the Thermodynamic Properties of Single Phases*; Goodwin, A. R. H., Marsh, K. N., Wakeham, W. A., Eds.; Elsevier: Amsterdam, 2003; pp 387–432.

- Callanan, J. E.; McDermott, K. M.; Westrum, E. F. Fusion of Mercury a New Certified Standard for Differential Scanning Calorimetry. *J. Chem. Thermodyn.* **1990**, *22*, 225–230.

- Osborne, N. S. Heat of Fusion of Ice. A Revision. *J. Res. Natl. Bur. Stand.* **1939**, *23*, 643–646.

- Laye, P. G. Differential Thermal Analysis and Differential Scanning Calorimetry. In *Principles of Thermal Analysis and Calorimetry*; Haines, P., Ed.; The Royal Society of Chemistry: Cambridge, U.K., 2002; pp 55–92.

(21) Paulechka, Y. U.; Blokhin, A. V.; Kabo, G. J.; Strechan, A. A. Thermodynamic Properties and Polymorphism of 1-alkyl-3-methylimidazolium bis(triflamides). *J. Chem. Thermodyn.* **2007**, *39*, 866–877.

(22) Fredlake, C. P.; Crosthwaite, J. M.; Hert, D. G.; Aki, S. N. V. K.; Brennecke, J. F. Thermophysical Properties of Imidazolium-Based Ionic Liquids. *J. Chem. Eng. Data* **2004**, *49*, 954–964.

(23) Tokuda, H.; Hayamizu, K.; Ishii, K.; Susan, M. A. B. H.; Watanabe, M. Physicochemical Properties and Structures of Room Temperature Ionic Liquids. 2. Variation of Alkyl Chain Length in Imidazolium Cation. *J. Phys. Chem. B* **2005**, *109*, 6103–6110.